の確立に向けたこれらの取り組みに貢献してきたわれわれの研究成果の一部と，それらの研究結果から帰納的に導き出された慢性影響評価研究の重要性について論ずる．

2. ナノマテリアルのリスク評価法の確立における課題

一般的に，化学物質の健康影響評価（リスクアセスメント）の基本的なフレームは，有害性評価と曝露評価，及び各々の評価内容を比較・統合化する過程のリスク判定のステップから成り立っている．この基本的なフレーム自体は，ナノマテリアルの健康影響評価に適用できるものであると考えられる．[1-5] しかし，ナノマテリアルに特徴的な新たな物理化学的性質，特にサイズが生体内高分子と近いことや，高い表面活性のために凝集し易い性質を考慮すると，よりサイズの大きい通常のバルク化合物や完全に溶解した単一分子化合物とは，生体内挙動が異なることが予想され，同じ化学組成の化合物であってもその毒性発現部位や発現様式は異なることが予想される．つまり，体内動態［吸収 absorption，分布 distribution，代謝 metabolism，排泄 excretion（ADME）］情報は，一般の化学物質より重要な意味を持つと考えられる．

そこで，生体内での挙動を把握するためには，生体試料中で検出，同定・定量できる方法を確立しなくてはならない．一般にナノマテリアルの開発段階において，その性質を把握するための物理化学的測定法も同時に開発されているはずであるが，それらの手法は生体試料中に存在するナノマテリアルにそのまま適用できないことも多い．さらに，機器分析法による生体試料中での検出や定量が可能になったとしても，生体内で実際にナノの状態で存在しているのか，あるいは再凝集などはしていないかなど，標的組織における最終的な生体内反応に影響を及ぼすと考えられる実際のナノマテリアルの存在状態を把握するためには，最終的には，組織標本の電子顕微鏡などによる確認が必要となる．

一方，体内動態に影響を与える因子として，投与法を検討する必要もある．単独では凝集し易いナノマテリアルをそのまま曝露するということは，物理的に巨大となった粒子は体への吸収性が低く，ナノマテリアル自体の体内動態や懸念される有害性を検出することが困難になると考えられるためである．そのために曝露実験時におけるナノマテリアルの分散手法の開発が必要となる．職業曝露などの比較的大量のナノマテリアル曝露の安全性を評価するという観点からは，凝集したままの曝露にも意義があるかもしれないが，製品中への混入や環境中への排出を経由した，分散された曝露も想定されることは考慮すべきであると考えられる．

Figure 1 は，凝集したナノマテリアルが，生体に取り込まれた場合に想定される体内動態を模式図化したものである．ナノマテリアルの使用用途にも依存するが，製品中のナノマテリアルはポリマー等の他の高分子化合物等と混合された状態，あるいはナノマテリアルだけが単独で製品から解離していく状態を考慮しても，この凝集性のために，大きな粒子として曝露する可能性が高いものと想定される．急性的には，このサイズの大きくなった物質は生体に取り込まれることはほとんどなく，局所的な刺激を起こすような変化を除いては，生体内で有害性が惹起される可能性は低いものと考えられる．しかし，仮に凝集したナノマテリアルが長期間に渡って，吸収部位である肺胞や消化管，損傷皮膚などの局所に滞留したり，慢性的に曝露したりするケースを想定すると，時間経過とともに小さくなった凝集体の粒子を除去するために，マクロファージなどの食細胞による取り込みや，表面活性の高いナノマテリアル分子と生体成分との結合作用による侵食作用により，生体に少しずつ取り込まれることが想定される．もしも生体内に取り込まれたナノマテリアルと生体内成分との結合性が高い場合には，容易に生体外に排出されることはなく，特定の組織等へ蓄積し易くなり，慢性影響の可能性を検討する必要が出てくると想定できる．

3. 国立医薬品食品衛生研究所における取り組みの成果の概要

以上のナノマテリアル固有の検討課題を考慮して，われわれは 2005 年より厚生労働科学研究の化学物質リスク研究事業の枠組みの中で，ナノマテリアルの健康影響評価手法の開発に係わる研究を推し進めてきたところである．われわれは，これらの検討課題を解決するために，Fig. 2 に示すように 4 つの項目を中心に研究を行ってきた．これらの項目の中で，*in vivo* 研究については，比較的研究初期の段階から中心的に取り組んできた．その中で，繊維

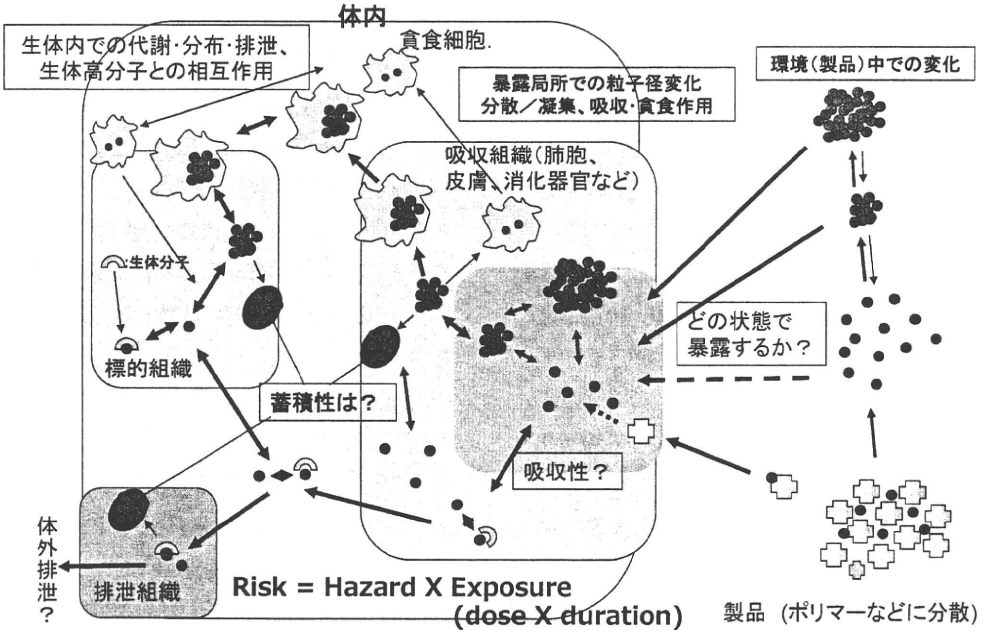

Fig. 1. The Estimated ADME Schema of Nanomaterials

*in vivo*試験法研究

MWCNTのP53ヘテロ欠失マウスへのi.p.投与による中皮腫誘発性を確認
バイオマーカとしてマウスのメソセリン抗体の作成
一方、C60の腹腔内投与による慢性的影響として腎臓への影響を示唆
TiO_2と C60の気管内投与による発がんプロモーション作用の示唆

吸入試験法研究

MWCNTのミスト暴露システムを開発
気管内投与時の分散性依存の発現様式差異を確認
リポソーム分散C60による気管内投与法を開発。

暴露測定法／動態解析研究

生体試料でのC60の定量的検出法との確立
静注後のC60の組織からの経時的消失検討
気管内投与後のMWCNTの肺及び肝臓での検出

*in vitro*試験法研究

細胞培養系でのリポソーム等を用いた分散法の確立
→C60やTiO_2の遺伝毒性、細胞透過性、
神経系の細胞機能への影響、などへの適用

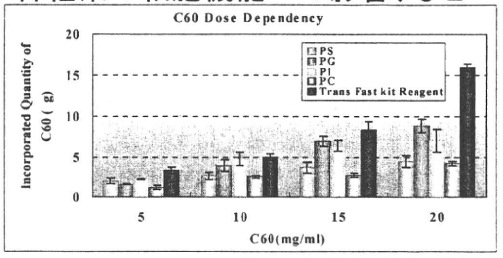

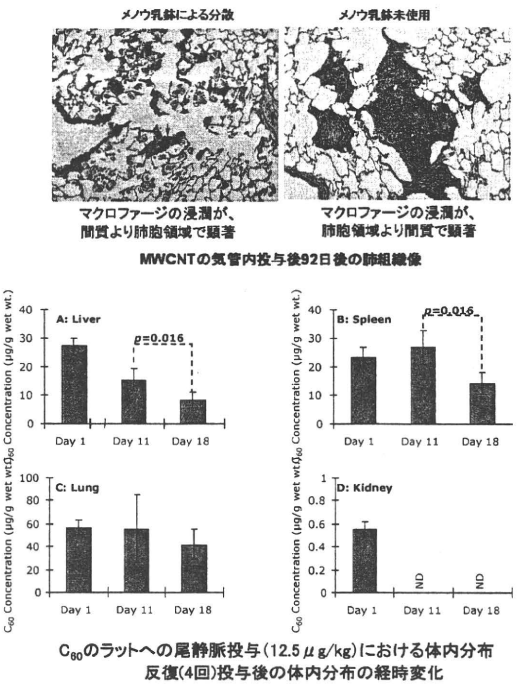

Fig. 2. The Overall Results of NIHS Projects for Nanomaterial Safety

長の長いタイプの多層型カーボンナノチューブ（MWCNT）が，中皮腫を誘発する可能性を持つことを確認した.[6] 上記の体内動態の重要性を考慮した概念からは，吸収性や体内分布について検証したのちに，慢性影響の可能性を検討することが論理的であるが，研究開始当時から，大量生産可能であった，酸化チタン（TiO_2）やフラーレン（C60），MWCNTについては，*in vivo* の慢性影響を先行して検討しておくべきであると判断した．特にその形状がアスベストに似ていたMWCNTについては，吸入曝露による有害影響が懸念されたが，MWCNTについての吸入曝露法が確立していない段階では，アスベストでも検証に使用されていた腹腔内投与による中皮腫誘発試験を行うこととした．

われわれの最初の実験は，アスベストで中皮腫の誘発時期が早くなることが知られているp53ヘテロノックアウトマウスへの腹腔内へ3 mg/mouseという高用量を投与することによって確認されたものであり，動物種の特異性や投与量の多さについて異論も指摘された．しかしその後の研究で，野生型の動物種であるF344ラットに対しても，同じMWCNTが中皮腫の誘発作用を持つことが確認された[7]ほか，投与量を1000分の1にまで少なくした実験においても中皮腫の起きることが示されている（投稿中）．

酸化チタンについては，雌ラットへの吸入曝露により発がん性のあることが示されているが，ナノサイズ化による発がん性の検証のために，気管内投与による肺がんのプロモーション作用の検討を行った．その結果，酸化チタンは，肺腺腫や乳腺腫に対してプロモーション作用を示し，その作用は，マクロファージから放出される炎症性因子であるMIP1αを介したものであることが示唆された.[8] 現在C60やMWCNTを用いたプロモーション作用の検討が進行中である．

一方，曝露手法の開発においては，ミスト法や粉体法によるMWCNTの吸入曝露システムの開発研究を進めているが，より簡易な手法として気管内投与のための適切な分散法の検討を行った．その結果，分散法の違いが肺の有害性発現様式に違いを引き起こすことを確認した.[9]

体内動態解析のために，生体試料中のC60やTiO_2の分析手法の開発や改良を行い，経口投与や気管内投与による体内吸収性について検討を行っている．現在のところ投与部位である消化管や肺以外で有意な検出量を確認できておらず，感度の向上に向けた研究を進めている．しかし，体内への吸収を前提にした解析として，C60の静脈内投与による解析を行ったところ，肝臓や脾臓，肺などへの分布を確認したが，腎臓への分布は極めて低いことが示された（投稿中）．その他，遺伝毒性や標的臓器などの毒性をスクリーニングするための *in vitro* 試験における培地等への分散法も検討対象としており，リポソームを用いたC60の分散法を確立した．

4. 慢性影響研究の重要性

ナノマテリアルの生体影響に関する情報はここ数年の活発な研究状況を反映して多くなりつつあるが，慢性影響に関する報告は依然その数が少ない状況である．一般の化学物質の有害性評価の常套手段として，変異原性試験や短期試験から情報を収集していくことは，必要なステップであり，OECDにおけるナノマテリアル作業グループの活動におけるスポンサーシッププログラムにおいても，加盟各国からの毒性試験情報として，短期試験を中心に収集されてきている．われわれの研究グループにおいても，これらの枠組みに対して，短期的な試験情報を中心に提供し始めている段階である．しかしMWCNTに関しては，研究初期から，短期毒性より長期毒性の方が懸念の強いことが，物性等の情報から推測されたところでもあり，その推定に基づいて，腹腔内投与の研究を最初にスタートさせた．腹腔内投与は，リスク評価の観点からは，曝露経路（吸入曝露）に伴う定量的な評価に問題のあるところであるが，最近の注目すべき研究として，分散剤で分散させたMWCNT（最高80 μgまで）をマウスに吸引させた研究や，MWCNT: 30 mg/m^{3}をマウスに単回吸入曝露した研究において，曝露後7–8週間目にMWCNTが胸膜に到達していたことが報告されている.[10,11] これらの研究結果は高用量の曝露による短期間の結果ではあるが，呼吸器を経由した曝露においてもMWCNTは胸膜（中皮）まで到達することを示唆しており，われわれの腹腔内投与による結果と合わせると，リスク評価の上でも重要な知見であると考えられる．

これらの腹腔内投与による中皮腫誘発能は，繊維状粒子による催腫瘍性のみを検出する系であり，短

いタイプやその他様々な形状のMWCNTにおける慢性毒性は別途検証する必要性がある．実際，われわれの行った腹腔内投与試験では，小さいサイズのナノチューブ繊維を含んだ細胞が腹膜の病変部のみならず，肝類洞内，又は肝葉間や腸間膜リンパ節の中にも認められ，体内に再分布することが示唆された（Fig. 3）.[6] さらに，SWCNTをマウスへ咽頭吸引させた実験では，一過性の急性症状の後に，炎症性細胞浸潤を伴わない間質の繊維化が認められている.[12] また，ApoEノックアウトマウスを用いた実験では，タンパクカルボニル化活性の変化を伴うミトコンドリアDNA障害と，アテローム性動脈硬化症の進行を増強することが示された.[13] MWCNTに関しても，マウスにMWCNT（200–400 μg）を気管内滴下した実験では，一過性の肺の炎症反応に加え，投与量に依存した血小板の活性化と凝固作用の活性化の促進が示唆されている.[14] また，MWCNTやSWCNTの気管内投与や経鼻投与により，アレルギー反応の増強反応が報告されている.[15–17] これらの結果が，カーボンナノチューブが直接体内循環に侵入した結果であるか，免疫細胞との接触を介した反応であるかを区別することは難しいが，曝露局所に留まらない全身作用の可能性を示している．われわれの酸化チタンの気管内投与による発がんプロモーション作用が，炎症因子により介在されたことは，これらの知見と同様の作用様式を示すものととらえることもできる．

以上の知見は，短期の試験だけでは検証することは困難であり，ナノマテリアルの有害性を確認するためには，長期の体内動態予測や慢性影響に関する研究が，重要なステップであることを示している．Figure 4にスクリーニング試験や確定試験を開発するための手順についてまとめた．通常の化学物質については，その長い歴史の中で明らかとなった有害性に対して，それぞれの毒性発現様式に応じてスクリーニング試験が開発され，現在まで運用されてきている．特に変異原性試験は発がん性を予測する試験としての重要な役割を担っている．しかし，現時点ではナノマテリアルによる有害性影響が，これまでの研究経験の中で明らかとなった影響だけに留まるのかについては，まだ誰も判定できない状況である．これまでの一般化学物質に対応する有害性とスクリーニング試験を活用して進めていくと同時に，未知の影響を見極める最初のステップとして，少な

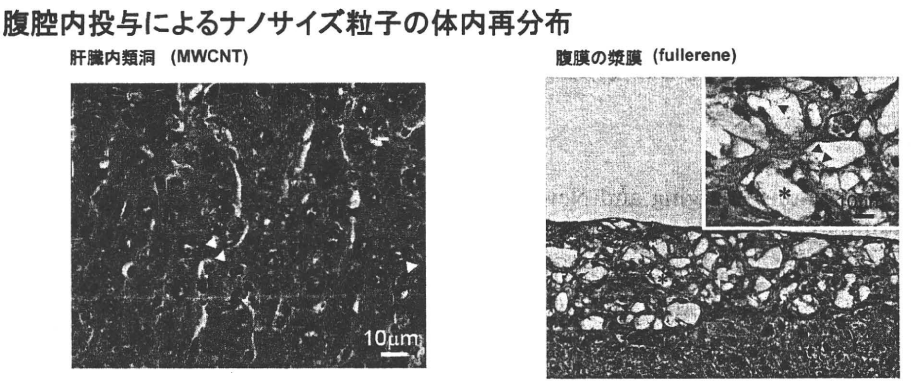

A. Takagi et al., J. Toxicol. Scie., **33**,105-116. (2008)

SWCNTやMWCNTによる全身性影響の示唆

•アテローム性動脈硬化症の進行の増強の可能性（ApoE$^{-/-}$マウス）
Z. Li *et al.*, *Environmental health perspectives*. **115**, 377-382 (2007)

•血小板の活性化と凝固作用の活性化（MWCNT気管内滴下）
A. Nemmar *et al.*, *J. Thrombosis, Haemostasis* **5:** 1217-1226 (2007)

•アレルギー反応の増強（MWCNT・SWCNT、気管内・経鼻投与）
E.J. Park *et al.*, *Toxicology*. **259**, 113-21 (2009)
U.C. Nygaard *et al.*, *Toxicol Sci*. **109**, 113-23 (2009)
K. Inoue *et al.*, *Toxicol Appl Pharmacol*. **237**, 306-16 (2009)

Fig. 3. The Suggestive Evidences for Systemic Toxicites by Nanomaterials

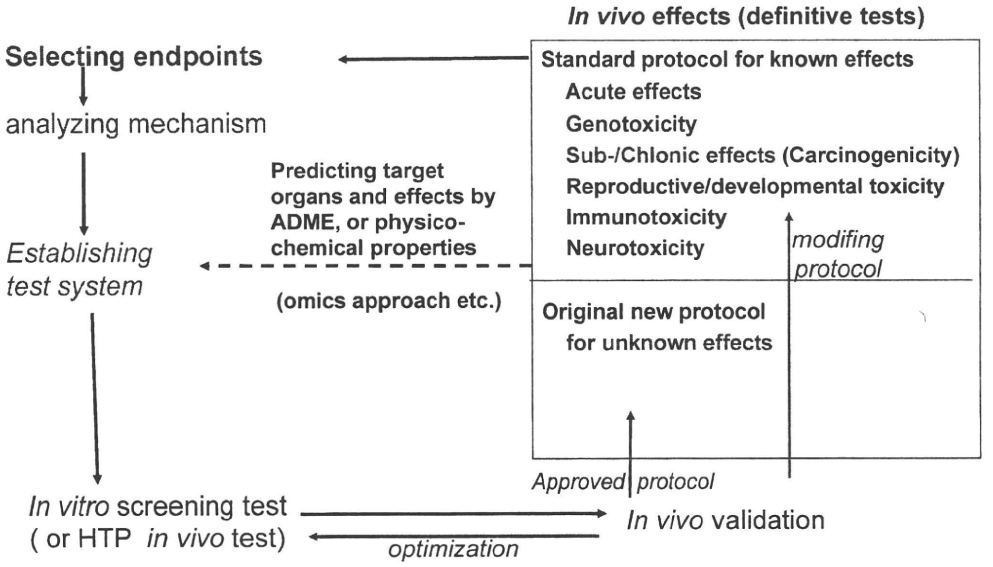

Fig. 4. The Schematic Development of Screening Tests and Definitive Tests

くとも代表的なナノマテリアルによる *in vivo* の慢性影響研究や，その影響を推定するためのナノマテリアルと生体成分との分子レベルでの相互作用や体内残留性様式の解析を進めていくべきであると考えられる．

謝辞 本稿で解説した研究成果の一部は，厚生労働科学研究費補助金（化学物質リスク研究事業）H17-化学-012，H18-化学--一般-007 及び H21-化学--一般-008 の助成によって行われたものです．

REFERENCES

1) Scientific Committee on Emerging and Newly Identified Health Risks, SCENIHR: ⟨http://ec.europa.eu/health/ph_risk/committees/04_scenihr/docs/scenihr_o_003b.pdf⟩, European Commission Web, cited 14 November, 2010.
2) Scientific Committee on Emerging and Newly Identified Health Risks, SCENIHR: ⟨http://ec.europa.eu/health/ph_risk/committees/04_scenihr/docs/scenihr_o_010.pdf⟩, European Commission Web, cited 14 November, 2010.
3) Food Safety Authority of Ireland, FSA, "The Relevance for Food Safety of Applications of Nanotechnology in Food and Feed Industries," Dublin, 2008.
4) UK Committees on Toxicity, Mutagenicity and Carcinogenicity of Chemicals in Food, Consumer Products and the Environment (COT, COM, COC): ⟨http://cot.food.gov.uk/pdfs/cotstatements2005nanomats.pdf⟩, COT Web, cited 14 November, 2010.
5) The Committee on Toxicity of Chemicals in Food, Consumer Products and the Environment: ⟨http://www.food.gov.uk/multimedia/pdfs/cotstatementnanomats200701.pdf⟩, cited 14 November, 2010.
6) Takagi A., Hirose A., Nishimura T., Fukumori N., Ogata A., Ohashi N., Kitajima S., Kanno J., *J. Toxicol. Sci.*, **33**, 105–116 (2008).
7) Sakamoto Y., Nakae D., Fukumori N., Tayama K., Maekawa A., Imai K., Hirose A., Nishimura T., Ohashi N., Ogata A., *J. Toxicol. Sci.*, **34**, 65–76 (2009).
8) Xu J., Futakuchi M., Iigo M., Fukamachi K., Alexander D. B., Shimizu H., Sakai Y., Tamano S., Furukawa F., Uchino T., Tokunaga H., Nishimura T., Hirose A., Kanno J., Tsuda H., *Carcinogenesis*, **31**, 927–935 (2010).
9) Wako K., Kotani Y., Hirose A., Doi T., Hamada S., *J. Toxicol. Sci.*, **35**, 437–446 (2010).
10) Nurkiewicz T. R., Porter D. W., Hubbs A. F., Stone S., Chen B. T., Frazer D. G., Boegehold M. A., Castranova V., *Toxicol. Sci.*, **110**, 191–203 (2009).
11) Ryman-Rasmussen J. P., Cesta M. F., Brody

A. R., Shipley-Phillips J. K., Everitt J. I., Tewksbury E. W., Moss O.R., Wrong B. A., Dodd D. F., Andersen M. E., Bonner J. C., *Nat. Nanotechnol.*, **4**, 747–751 (2009).

12) Shvedova A. A., Kishin E. R., Mercer R., Murray A. R., Johnson V. J., Potapovich A. I., Tyurina Y. Y., Gorelik O., Arepalli S., Schwegler-Berry D., Hubbs A. F., Antonini J., Evans D. E., Ku B. K., Ramsey D., Maynard A., Kagan V. E., Castranova V., Baron P., *Am. J. Physiol. Lung cell. mol. physiol.*, **289**, L698–L708 (2005).

13) Li Z., Hulderman T., Salmen R., Chapman R., Leonars S. S., Young S. H., Shvedova A., Luster M. I., Simeonove P. P., *Environ. Health Perspect.*, **115**, 377–382 (2007).

14) Nemmar A., Hoet P. H., Vandervoort P., Dinsdale D., Nemery B., Hoylaerts M. F., *J. Thromb. Haemost.*, **5**, 1217–1226 (2007).

15) Park E. J., Cho W. S., Jeong J., Yi J., Choi K., Park K., *Toxicology*, **259**, 113–121 (2009).

16) Nygaard U. C., Hansen J. S., Samuelsen M., Alberg T., Marioara C. D., Løvik M., *Toxicol. Sci.*, **109**, 113–123 (2009).

17) Inoue K., Koike E., Yanagisawa R., Hirano S., Nishikwa M., Takano H., *Toxicol. Appl. Pharmacol.*, **237**, 306–316 (2009).

The Journal of Toxicological Sciences (J. Toxicol. Sci.)
Vol.35, No.2, 265-270, 2010

Letter

Serum level of expressed in renal carcinoma (ERC)/ mesothelin in rats with mesothelial proliferative lesions induced by multi-wall carbon nanotube (MWCNT)

Yoshimitsu Sakamoto[1], Dai Nakae[1,2], Yoshiaki Hagiwara[3,4], Kanako Satoh[1], Norio Ohashi[1], Katsumi Fukamachi[5], Hiroyuki Tsuda[5], Akihiko Hirose[6], Tetsuji Nishimura[7], Okio Hino[3] and Akio Ogata[1]

[1]Department of Environmental Health and Toxicology, Tokyo Metropolitan Institute of Public Health, 3-24-1 Hyakunin'cho, Shin'juku-ku, Tokyo 169-0073, Japan
[2]Tokyo University of Agriculture, 1-1-1 Sakuragaoaka, Setagaya-ku, Tokyo, 156-8502, Japan
[3]Department of Pathology and Oncology, Juntendo University School of Medicine, 2-1-1 Hongo, Bunkyo-ku, Tokyo 113-8421, Japan
[4]Immuno-Biological Laboratory Co., Ltd., 1091-1 Naka, Fujioka, Gunma 375-0005, Japan
[5]Department of Molecular Toxicology, Nagoya City University, 1 Kawasumi, Mizuho-cho, Mizuho-ku, Nagoya, Aichi 467-8601, Japan
[6]Divisions of Risk Assessment, Biological Safety Research Center and [7]Environmental Chemistry, National Institute of Health Sciences, 1-18-1 Kamiyoga, Setagaya-ku, Tokyo 158-8501, Japan

(Received November 5, 2009; Accepted December 30, 2009)

ABSTRACT — Expressed in renal carcinoma (ERC)/mesothelin is a good biomarker for human mesothelioma and has been investigated for its mechanistic rationale during the mesothelioma development. Studies are thus ongoing in our laboratories to assess expression of ERC/mesothelin in sera and normal/proliferative/neoplastic mesothelial tissues of animals untreated or given potentially mesothelioma-inducible xenobiotics, by an enzyme-linked immunosorbent assay (ELISA) for N- and C-(terminal fragments of) ERC/mesothelin and immunohistochemistry for C-ERC/mesothelin. In the present paper, we intend to communicate our preliminary data, because this is the first report to show how and from what stage the ERC/mesothelin expression changes during the chemical induction of mesothelial proliferative/neoplatic lesions. Serum N-ERC/mesothelin levels were 51.4 ± 5.6 ng/ml in control male Fischer 344 rats, increased to 83.6 ± 11.2 ng/ml in rats given a single intrascrotal administration of 1 mg/kg body weight of multi-wall carbon nanotube (MWCNT) and bearing mesothelial hyperplasia 52 weeks thereafter, and further elevated to 180 ± 77 ng/ml in rats similarly treated and becoming moribund 40 weeks thereafter, or killed as scheduled at the end of week 52, bearing mesothelioma. While C-ERC/mesothelin was expressed in normal and hyperplastic mesothelia, the protein was detected only in epithelioid mesothelioma cells at the most superficial layer. It is thus suggested that ERC/mesothelin can be used as a biomarker of mesothelial proliferative lesions also in animals, and that the increase of levels may start from the early stage and be enhanced by the progression of the mesothelioma development.

Key words: Serum mesothelin, Rat, MWCNT, Mesothelial proliferative lesions

INTRODUCTION

Mesothelioma is a highly aggressive malignant tumor and developed in people previously exposed to asbestos, after a long latency period of 30-40 years. It is desired to establish a biomarker that can identify potential patients with early stage tumors or even as yet without tumors among the high-risk population.

Expressed in renal carcinoma (ERC)/mesothelin is a product of the *Erc* gene discovered in renal carcinomas of the Eker rats (Hino *et al.*, 1995) and confirmed as a homolog of the human *mesothelin/megakaryocyte poten-*

Correspondence: Yoshimitsu Sakamoto (E-mail: Yoshimitsu_Sakamoto@member.metro.tokyo.jp)

ciating factor gene (Hino, 2004; Yamashita *et al.*, 2000). A 71-kDa glycosylphosphatidylinositol anchor-type membranous protein is produced and physiologically cleaved by a furin-like protease to yield a membrane-binding 40-kDa C-terminal (C-ERC/mesothelin) and a secreting 31-kDa N-terminal (N-ERC/mesothelin) fragments (Chang and Pastan, 1996; Maeda and Hino, 2006; Yamaguchi, *et al.*, 1994). ERC/mesothelin is a useful marker for human mesothelioma cases (Hino *et al.*, 2007; Maeda and Hino, 2006) and its specific enzyme-linked immunosorbent assay (ELISA) system has been developed (Hagiwara *et al.*, 2008; Nakaishi *et al.*, 2007) for the clinical use (Maeda and Hino, 2006; Shiomi, *et al.*, 2006, 2008; Tajima *et al.*, 2008). The most important question is as to whether ERC/mesothelin can be efficient also in the early phase of the mesothelioma development, and studies are ongoing in our laboratories to assess ERC/mesothelin levels in animals untreated or given potentially mesothelioma-inducible xenobiotics.

We preliminarily assessed ERC/mesothelin levels using the samples of our previous study demonstrating the induction of mesothelial proliferative lesions in male Fisher 344 rats given multi-wall carbon nanotube (MWCNT) (Sakamoto *et al.*, 2009) In the present paper, we intend to communicate this preliminary data, despite its very limited sample numbers, because this is the first report to show how and from what stage the ERC/mesothelin expression changes during the chemical induction of mesothelial proliferative/neoplatic lesions.

MATERIALS AND METHODS

Ethical consideration of the experiments

An experimental protocol was approved by the Experiments Regulation/Animal Experiment Committees of the Tokyo Metropolitan Institute of Public Health for its scientific and ethical appropriateness, including concern for animal welfare, with strict obedience to domestically and internationally applicable declarations, laws, guidelines and rules.

Samples

Male Fisher 344 rats were purchased at their age of 4 weeks old from Charles River Laboratories Japan Inc. (Kanagawa, Japan) and maintained in our animal room (24-25°C, 50-60% relative humidity, 10 times/hr air ventilation and 12-hr light/dark cycle) until use.

Normal rat samples

Serum samples were obtained from 3, 1 and 2 untreated rats at their ages of 11, 42 and 81 weeks old, respectively.

Vehicle/MWCNT-treated rat samples

As detailed elsewhere (Sakamoto *et al.*, 2009), rats were given a single intrascrotal administration of 1 ml/kg body weight of vehicle (2% carboxymethylcellulose) or 1 mg/kg body weight of MWCNT at the age of 12 weeks old and left untreated for up to 52 weeks. In the present study, 9 samples were used: 3 from vehicle-treated rats killed as scheduled at the end of week 52, without any mesothelial changes; 3 from MWCNT-treated rats similarly killed, with mesothelial hyperplasias but without mesotheliomas; and 3 from other MWCNT-treated animals, 1 killed as moribund at week 40 and 2 killed as scheduled at the end of week 52, with early and advanced stages mesotheliomas and hemorrhagic ascites. Serum samples and in the last case an ascites sample were obtained at the time of the autopsy, and 10% neutrally buffered formalin-fixed, paraffin-embedded, mesothelial tissue samples were routinely prepared.

ERC/mesothelinin ELISA assay

Serum and ascites ERC/mesothelin levels were analyzed using rat N- and C-ERC/mesothelin assay kits (Immuno-Biological Laboratories [IBL] Co., Ltd., Gunma, Japan) adapting from the method of Hagiwara *et al.* (2008), the detection limit being 0.1 ng/ml. A 6-µl aliquot was diluted with 234 µl of phosphate-buffered saline containing 1% bovine serum albumin and 0.05% Tween 20. Assays were conducted according to the manufacturer' instruction to measure an optical density at 450 nm. Each sample was assessed in duplicate.

Histology and C-ERC/mesothelin immunohistochemistry

Two serial, 4-µm-thick sections were prepared and deparaffinized. One was processed through a routine hematoxylin and eosin (HE) staining procedure and hisgtologically examined. The other was heated in 10 mM citrate buffer, pH 6.0, treated with 3% hydrogen peroxide, incubated with a primary anti-rat C-ERC/mesothelin antibody (IBL) overnight at 4°C, washed with tris-buffered saline, and re-incubated using an Envision system (DAKO Japan Company, Limited, Tokyo, Japan). Signals were visualized by 3,3'-diaminobenzidine, and the sections were counter-stained with hematoxylin.

Statistical analysis

Statistical significance of intergroup difference for the N-ERC/mesothelin level was assessed using Student's *t*-test, and *p*-values less than 0.05 were considered significant.

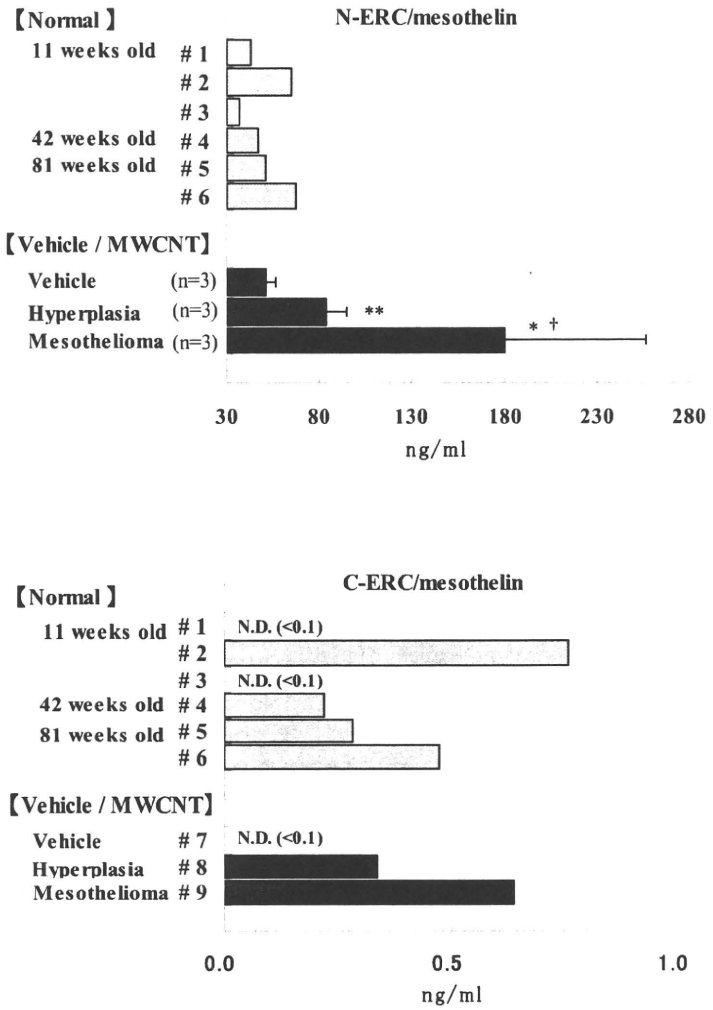

Fig. 1. Serum levels of A, N-ERC/mesothelin and B, C-ERC/mesothelin. Each data is a mean of duplicate assays. #1- #6 in Fig. A and #1- #9 in Fig. B show sample numbers. "N.D.", not detectable, indicates that the data was below the detection limit of 0.10 ng/ml. Values of N-ERC/mesothelin of samples from vehicle, hyperplasia and mesothelioma groups in Fig. B represent the means ± S.D. (n = 3).
Statistical significant difference by Student's t-test: $^{*}P < 0.05$, $^{**}P < 0.01$ as compared from the vehicle group and $^{\dagger}P < 0.05$ as compared from the hyperplastic group.

RESULTS AND DISCUSSION

Serum N-ERC/mesothelin levels of the normal rats were 43.4, 65.1 and 37.3 ng/ml, 47.1 ng/ml and 51.1 and 67.5 ng/ml; while those of C-ERC/mesothelin were < 0.1, 0.8 and < 0.1 ng/ml, 0.2 ng/ml and 0.3 and 0.5 ng/ml; for 11, 42 and 81 weeks of their ages, respectively (Fig. 1). These were respectively within the same range, and the N-ERC/mesothelin levels were substantially higher than the C-ERC/mesothelin levels. No apparent age-dependent changes were obtained for either fragment.

Serum N-(n = 3) and C-(n = 3) ERC/mesothelin levels of the vehicle-treated rat was 51.4 ± 5.6 ng/ml and < 0.1 ng/ml, respectively, within the normal ranges, whereas serum N-ERC/mesothelin levels of MWCNT-treated rats were increased by the induction of mesothelial hyperpla-

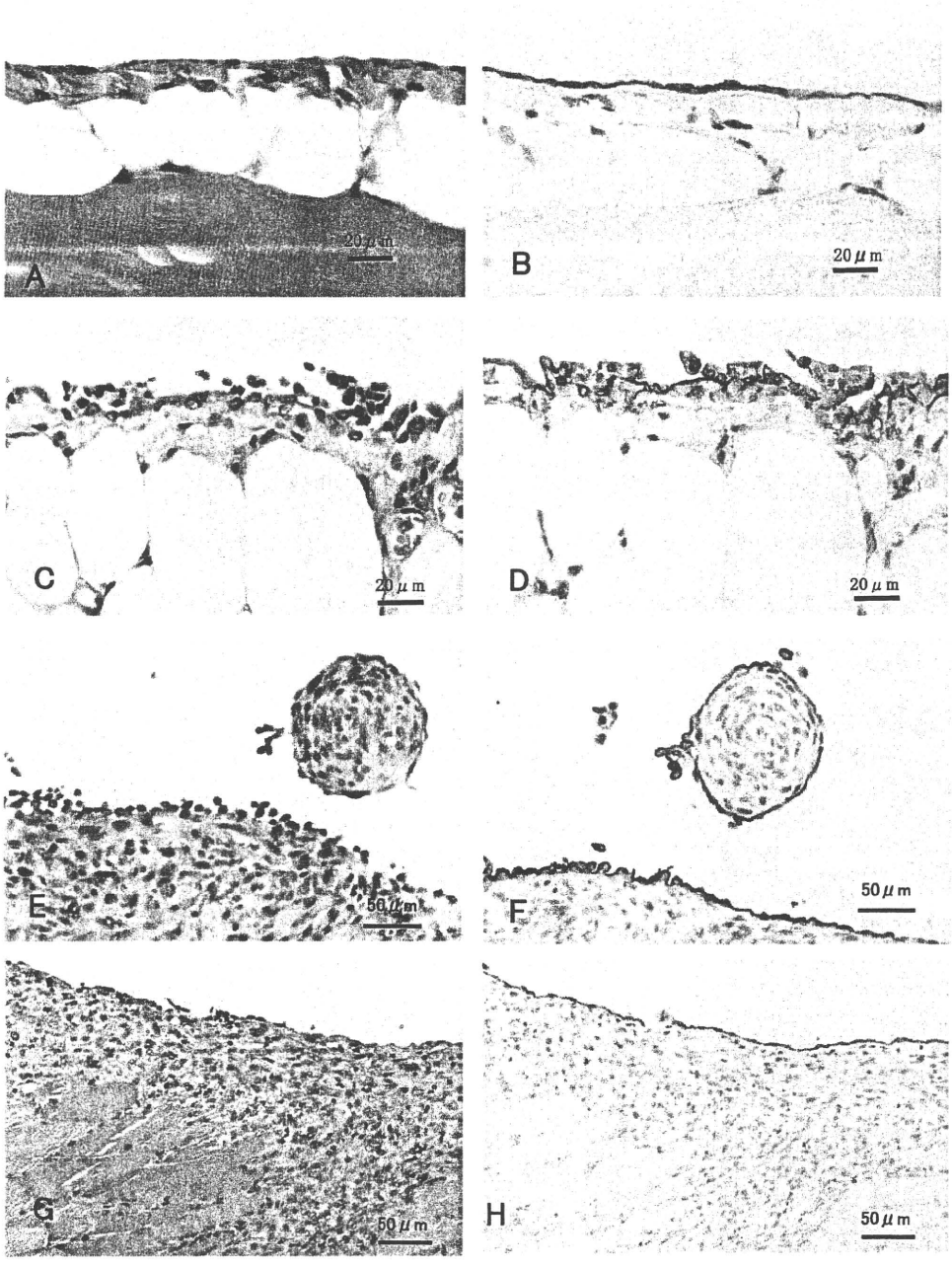

Fig. 2. Representative histology and C-ERC/mesothelin immunohistochemistry.
A, intact mesothelia in the parietal peritoneum of the vehicle-treated rat, HE; B, A's serial section, C-ERC/mesothelin; C, a mesothelial hyperplasia in the retroperotineal fat tissue of the MWCNT-treated rat, HE; D, C's serial section, C-ERC/mesothelin; E, an early-stage epithelioid/polypoid type mesothelioma in retroperotineal fat tissue of the other MWCNT-treated rat, HE; F, E's serial section, C-ERC/mesothelin; G, an advanced-stage mostly-sarcomatoid/invasive-nodular type mesothelioma in the diaphragm of the MWCNT-treated rat (the same animal as E/F), HE; H, G's serial section, C-ERC/mesothelin. Bars with their lengths are inserted to indicate magnifications.

sia (83.6 ± 11.2 ng/ml) and further by that of mesothelioma (179 ± 77 ng/ml; 3,004 ± 665 ng/ml in ascites) (Fig. 1). Serum N-ERC/mesothelin levels in experimental animals have only been assessed in Eker and Wistar rats and nude mice, untreated or transplanted with a rat mesothelioma cell line, MetEt-40 (Hagiwara *et al.*, 2008; Nakaishi *et al.*, 2007). The present data for the first time demonstrates that serum N-ERC/mesothelin level was increased already at the stage of preneoplastic, mesothelial hyperplasia and further increased by the chemical induction of mesothelioma. This may be in line with the recent findings that elevated serum mesothelin is detected before the development of grossly visible carcinoma lesions in a rat pancreatic carcinoma models (Fukamachi *et al.*, 2009). In human mesothelioma, it has been reported that N-ERC/mesothelin level increased with the stage went up of epithelioide type mesothelioma in human case (Shiomi *et al.*, 2008). It is not known, however, how N-ERC/mesothelin levels change in the stage of preneoplasia at this moment. Large-scaled, detailed investigations using the MWCNT-mesothelioma model are ongoing in our laboratories.

Serum C-ERC/mesothelin levels of MWCNT-treated rats were 0.4 and 0.6 ng/ml, within the normal/vehicle range (Fig. 1B). This is in accordance with the previous finding in nude mice transplanted with MetET-40 (Hagiwara *et al.*, 2008), and can be attributed to the membrane-binding property of C-ERC/mesothelin (Maeda and Hino, 2006). Ascites level of C-ERC/mesothelin in the mesothelioma case was slightly increased to 10.9 ng/ml (Fig. 1B). This is speculated to result from a release of C-ERC/mesothelin by phosphatidylinositol-specific phospholipase C (Chang and Pastan, 1996) or a contamination of desquamated mesothelioma cells.

Immuohistochemical C-ERC/mesothelin signals were constantly detected in cell membranes. C-ERC/mesothelin was detected in intact (Figs. 2A and B) and hyperpastic (Figs. 2C and D) mesothelia. Taken the ELISA data together, it might be possible that the ERC/mesothelin level starts increased from the preneoplastic stage.

C-ERC/mesothelin was found only in epithelioid (mesothelioid) tumor cells present at the most superficial layer of early-stage, epithelioid/polypoid (Figs. 2E and F) and advanced-stage, mostly-sarcomatoid/invasive-nodular (Figs. 2G and H) types of mesotheliomas. In humans, epithelioid types, but not sarcomatoid types or sarcomatoid components of biphasic (mixed) types, immunohistochemically express C-ERC/mesothelin (Chang and Pastan, 1996; Shiomi *et al.*, 2008; Ordóñez, 2003). Accordingly, serum N-ERC/mesothelin levels were only slightly increased or often unchanged in sarcomatoid and biphasic types, in contrast to the epithelioid type (Hassan *et al.*, 2006; Shiomi *et al.*, 2008). The present findings suggest that the increaseof ERC/mesothelin levels in mesotheliomas may be a universal event for all types and stages, and that C-terminal fragments may become unproduced or changed its tertiary structure and/or epitope construction by the neoplastic conversion.

In conclusion, the present data suggests that ERC/mesothelin can be used as a biomarker of mesothelial proliferative lesions also in animals, and that its increase of its levels may start from the early stage and be enhanced by the progression of the mesothelioma development.

ACKNOWLEDGMENTS

This work was supported in part by a research budget of the Tokyo Metropolitan Government, Japan, and Grants-in-Aid for Scientific Research from the Ministry of Health, Labour and Welfare of Japan, from the Japan Society for the Promotion of Science, and from the Ministry of Education, Culture, Sports, Science and Technology of Japan. This study was also partially supported by a consignment expense for Molecular Imaging Program on "Research Base for PET Diagnosis" from the Ministry of Education, Culture, Sports, Science and Technology of Japan.

REFERENCES

Chang, K. and Pastan, I. (1996): Molecular cloning of mesothelin, a differentiation antigen present on mesothelium, mesotheliomas, and ovarian cancers. PNAS USA, **93**, 136-140.

Fukamachi, K., Tanaka, H., Hagiwara, Y., Ohara, H., Joh, T., Iigo, M., Alexander, D.B., Xu, J., Long, N., Takigahira, M., Yanagihara, K., Hino, O., Saito, I. and Tsuda, H. (2009): An animal model of preclinical diagnosis of pancreatic ductal carcinomas. Biochem. Biophys. Res. Commun., **390**, 636-641.

Hagiwara, Y., Hamada, Y., Kuwahara, M., Maeda, M., Segawa, T., Ishikawa, K. and Hino, O. (2008): Establishment of a novel specific ELISA system for rat N- and C-ERC/mesothelin. Rat ERC/mesothelin in the body fluids of mice bearing mesothelioma. Cancer Sci., **99**, 666-670.

Hassan, R., Remaley, A.T., Sampson, M.L. Zhang, J., Cox, D.D., Pingpank, J., Alexander, R., Willingham, M., Pastan, I. and Onda, M. (2006): Detection and quantitation of serum mesothelin, a tumor marker for patients with mesothelioma and ovarian cancer. Clin. Cancer Res., **12**, 447-453.

Hino, O., Kobayashi, E., Nishizawa, M., Kubo, Y., Kobayashi, T., Hirayama, Y., Takai, S., Kikuchi, Y., Tsuchiya, H., Orimoto, K., Kajino, K., Takahata, T. and Hitani, H. (1995): Renal carcinogenesis in the Eker rat. J. Cancer Res. Clin. Oncol., **121**, 602-605.

Hino, O. (2004): Multistep renal carcinogenesis in the Eker (*Tsc2* gene mutant) rat model. Curr. Mol. Med., **4**, 807-811.

Hino, O., Shiomi, K. and Maeda, M. (2007): Diagnostic biomarker of asbestos-related mesothelioma: example of translational research. Cancer Sci., **98**, 1147-1151.

Maeda, M. and Hino, O. (2006): Molecular tumor markers for asbestos-related mesothelioma: serum diagnostic markers. Pathol. Int., **56**, 649-654.

Ordóñez, N.G. (2003): Value of mesothelin immunostaining in the diagnosis of mesothelioma. Mod. Pathol., **16**, 192-197.

Nakaishi, M., Kajino, K., Ikesue, M., Hagiwara, Y., Kuwahara, M., Mitani, H., Horikoshi-Sakuraba, Y., Segawa, T., Kon, S., Maeda, M., Wang, T., Abe, M., Yokoyama, M. and Hino, O. (2007): Establishment of the enzyme-linked immunosorbent assay system to detect the amino terminal secretary form of rat Erc/Mesothelin. Cancer Sci., **98**, 659-664.

Sakamoto, Y., Nakae, D., Fukumori, N., Tayama, K., Maekawa, A., Imai, K., Hirose, A., Nishimura, T., Ohashi, N. and Ogata, A. (2009): Induction of mesothelioma by a single intrascrotal administration of multi-wall carbon nanotube in intact male Fischer 344 rats. J. Toxicol. Sci., **34**, 65-76.

Shiomi, K., Miyamoto, H., Segawa, T., Hagiwara, Y., Ota, A., Maeda, M., Takahashi, K., Masuda, K., Sakao, Y. and Hino, O. (2006): Novel ELISA system for detection of N-ERC/mesothelin in the sera of mesothelioma patients. Cancer Sci., **97**, 928-932.

Shiomi, K., Hagiwara, Y., Sonoue, K., Segawa, T., Miyashita, K., Maeda, M., Izumi, H., Masuda, K., Hirabayashi, M., Moroboshi, T., Yoshiyama, T., Ishida, A., Natori, Y., Inoue, A., Kobayashi, M., Sakao, Y., Miyamoto, H., Takahashi, K. and Hino, O. (2008): Sensitive and specific new enzyme-linked immunosorbent assay for N-ERC/mesothelin increases its potential as a useful serum tumor marker for mesothelioma. Clin. Cancer Res., **14**, 1431-1437.

Tajima, K., Hirama, M., Shiomi, K., Ishiwata, T., Yoshioka, M., Iwase, A., Iwakami, S., Yamazaki, M., Toba, M., Tobino, K., Sugano, K., Ichikawa, M., Hagiwara, Y., Takahashi, K. and Hino, O. (2008): ERC/mesothelin as a marker for chemotherapeutic response in patients with mesothelioma. Anticancer Res., **28**, 3933-3936.

Yamaguchi, N., Hattori, K., Oheda, M., Kojima, T., Imai, N. and Ochi, N. (1994): A novel cytokine exhibiting megakaryocyte potentiating activity from a human pancreatic tumor-cell line HPC-Y5. J. Biol. Chem., **269**, 805-808.

Yamashita, Y., Yokoyama, M., Kobayashi, E., Takai, S. and Hino, O. (2000): Mapping and determination of the cDNA sequence of the *Erc* gene preferentially expressed in renal cell carcinoma in the *Tsc2* gene mutant (Eker) rat model. Biochem. Biophys. Res. Commun., **275**, 134-140.

Genes and Environment, Vol. 33, No. 1 pp. 27–31 (2011)

Short communication

Fullerene (C_{60}) Is Negative in the *In Vivo Pig-A* Gene Mutation Assay

Katsuyoshi Horibata[1,5], Akiko Ukai[1], Naoki Koyama[1], Atsuya Takagi[2], Jun Kanno[2], Takafumi Kimoto[3], Daishiro Miura[3], Akihiko Hirose[4] and Masamitsu Honma[1]

[1]Division of Genetics and Mutagenesis, National Institute of Health Sciences, Tokyo, Japan
[2]Division of Toxicology, National Institute of Health Sciences, Tokyo, Japan
[3]TEIJIN Pharma Limited, Tokyo, Japan
[4]Division of Risk Assessment, National Institute of Health Sciences, Tokyo, Japan

(Received December 24, 2010; Revised January 20, 2011; accepted January 21, 2011)

Carbon nanoparticles, such as carbon nanotubes and fullerene (C_{60}), are potential candidates as leading substances in nanotechnological fields, but little is known about their safety. Here we examined *in vivo* genotoxicity of C_{60}, by performing the *Pig-A* gene mutation assay in the peripheral blood of male C57BL/6Cr mice. Mice were given single intraperitoneal injection of 3 mg of C_{60} particles in 0.5 mL suspension containing 0.1%-Tween80-saline. As a positive control for the *Pig-A* gene mutation assay, mice were given a single oral administration of *N*-nitroso-*N*-ethylurea. At 2 and 8 weeks after treatments, we analyzed CD24-negative and -positive red blood cells in peripheral blood and calculated *Pig-A* mutant frequencies. As a result, we detected no significant differences in the mutant frequencies between C_{60} treated and non-treated mice, indicating that C_{60} is negative for genotoxicity *in vivo* in the limited target tissues assessed in this study. For the full assessment, we need comprehensive whole body survey on the genotoxicity of C_{60}.

Key words: carbon nanoparticle, *in vivo* genotoxicity, *Pig-A* gene mutation assay, fullerene

Introduction

Manufactured nanomaterials are important substances in nanotechnology, and the potential human and environmental risks need to be investigated for risk assessment and management.

There are several reports on the toxicities induced by carbon nanoparticles, such as single-wall carbon nanotubes (SWCNTs), multi-wall carbon nanotubes (MWCNTs) and fullerene (C_{60}). Intraperitoneal application of MWCNTs induced mesothelioma in $p53^{+/-}$ mouse (1) and intrascrotal administration of MWCNTs induced mesothelioma in wild-type rats (2). Reports on the *in vivo* genotoxicity of C_{60}, however, are conflicting. It was reported that intratracheal instillation of C_{60} increased both mutation frequency detected by *gpt*-assay and DNA damage detected by comet assay in lung (3). Nevertheless another group showed that treatment with C_{60} by gavage has no genotoxical effect in ICR mice, using *in vivo* micronucleus test in bone marrow cells (4). These discrepancies could have been caused by differences in administration route, test method, or target organ.

Here we examined the *in vivo* genotoxicity of C_{60} using a different test system—the recently established *Pig-A* gene mutation assay (5,6). The *Pig-A* assay, a powerful tool for the evaluation of *in vivo* genotoxicity, is based on flow cytometric enumeration of glycosylphosphatidylinositol (GPI) anchor-deficient erythrocytes and has been shown to be applicable across species from rodent to monkey (5–8). With this method, we need no transgenic animals to test *in vivo* genotoxicity, but need only 1–2 μL peripheral blood (5,6). Additionally, long-term, accumulated *in vivo* genotoxic effects could be evaluated (9).

Materials and Methods

Test chemicals: Fullerene (C_{60}, Nanom purple SUH; purity >99.9%, Frontier Carbon Corporation, Tokyo, Japan) was obtained and prepared as previously described with some modifications (1). Briefly, C_{60} was suspended to physiological saline (Ohtsuka Pharmaceutical Co., Tokyo, Japan) and autoclaved. After addition of Tween 80 (Polysorbate 80 (HX), NOF Corporation, Tokyo, Japan) at a final concentration of 0.1%, solutions were subjected to sonication by ultrasonic homogenizer (VP30s, TAITEC Co. Japan). C_{60} was prepared at a final concentration of 6 mg/mL. *N*-nitroso-*N*-ethylurea (ENU, Sigma) was dissolved in PBS (pH

[5]Correspondence to: Katsuyoshi Horibata, Division of Genetics and Mutagenesis, National Institute of Health Sciences, 1-18-1 Kamiyoga, Setagaya-ku, Tokyo 158-8501, Japan. Tel: +81-3-3700-1141, Fax: +81-3-3700-2348, E-mail: horibata@nihs.go.jp

6.0) at 10 mg/mL as previously described (5).

Animal treatment: Mice were treated as described previously (1). In brief, 6 male wild-type C57BL/6Cr mice (SLC, Shizuoka, Japan) at the age of 9–11 weeks were given single i.p. injection of 3 mg/head suspension (0.5 mL) of C_{60}. Vehicle solution (0.5 mL) was given to 6 mice as negative controls. As a positive control of this study, 5 mice were given single oral administration of ENU (40 mg/kg). Peripheral bloods were withdrawn from tail vein of mice and analyzed by the *Pig-A* gene mutation assay. All mice were housed individually under specific pathogen-free conditions, with a 12 h light-dark cycle at the animal facility of NIHS. All mice were given tap water and gamma-ray irradiated CRF-1 pellets (Oriental Yeast Co., ltd.) *ad libitum*. Animal experiments were humanely conducted under the regulation and permission of the Animal Care and Use Committee of the National Institute of Health Sciences, Tokyo, Japan.

Antibodies: Anti-mouse TER119 antibody for erythroid cells staining (clone TER-119, PE-Cy7-conjugated) and anti-mouse CD24 antibody (clone M1/69, FITC-conjugated) were obtained from BioLegend.

***Pig-A* gene mutation assay in mice:** Mice *Pig-A* gene mutation assay was performed as previously described (5,8), with some modifications. In brief, EDTA/2K was dissolved in distilled water to make a 12% solution, and used as an anticoagulant. Eighteen μL of peripheral blood were mixed with 2 μL of EDTA solution. Two μL of blood/EDTA mixture was suspended in 0.2 mL of PBS, and the cells were labeled with 1 μg of each anti-mouse TER119 and anti-mouse CD24 antibodies. After incubation for 1 h in the dark at room temperature, the cells were washed once by centrifugation ($500 \times g$, 5 min), resuspended in 2 mL of PBS, and examined using a FACS Canto II flow cytometer (BD Biosciences). After gating for single cells, about 1,000,000 TER119-positive cells were analyzed for the presence of CD24 on their surface. The data were statistically compared with the corresponding solvent control using the Student's t-test.

Results

***Pig-A* gene mutation assay with mice peripheral blood:** Recent works provided that the erythrocyte-based *Pig-A* gene mutation assay is applicable across species (5–8). According to these reports, we modified the original *Pig-A* gene mutation assay and performed it with mice peripheral blood. To classify white blood cells (WBCs) and red blood cells (RBCs) in mice peripheral blood, RBCs were stained with anti-TER119 antibody. Anti-CD24 antibody was used to detect GPI-anchored protein as previously reported (8,10). The gating strategy that was used to score GPI anchor deficient RBCs population was shown in Fig. 1. Single cells including RBCs and WBCs were gated by light scatter (Fig. 1A). To exclude WBCs from this population, TER119-positive cells (Fig. 1B) were analyzed further for the presence on the cell surface of either the GPI-anchored CD24 (Fig. 1C and 1D). The gate used for CD24-negative cells was established by blood cell samples prepared without the fluorescent reagents.

***In vivo* genotoxicity tests on fullerene (C_{60}) analyzed by the *Pig-A* gene mutation assay:** At 2 and 8 weeks after the injection of C_{60} (3 mg/head) and ENU, we analyzed CD24-negative and -positive RBCs in peripheral blood. At both 2 and 8 weeks after the injection, higher amounts of CD24 deficient RBCs were observed in the ENU treated mice (Fig. 1D) as compared with the solvent control (not shown) and C_{60} treated mice (Fig. 1C), respectively. Frequencies of CD24-negative RBCs were summarized in Fig. 2. Frequency of CD24-negative RBCs was significantly increased in ENU treated mice (2 weeks after treatment; $30.12 \pm 3.54 \times 10^{-6}$, and 8 weeks after treatment; $36.64 \pm 15.71 \times 10^{-6}$). However, we detected no obvious differences in frequency of CD24-negative RBCs between C_{60} treated and non-treated mice ($0.25 \pm 0.30 \times 10^{-6}$ versus $0.42 \pm 0.19 \times 10^{-6}$ after 2 weeks and $0.82 \pm 0.54 \times 10^{-6}$ versus $1.87 \pm 1.51 \times 10^{-6}$ after 8 weeks).

These results indicated that although the *Pig-A* gene mutation assay with mouse peripheral blood was appropriately performed, C_{60} was negative for genotoxicity *in vivo* in the RBCs assessed in our study.

Discussion

We demonstrated here that C_{60} (3 mg/head) given intraperitoneally to male C57BL/6Cr mice was negative in the *Pig-A* gene mutation assay using peripheral blood, suggesting that C_{60} was not mutagenic to erythroid precursor cells or hematopoietic stem cells.

The *Pig-A* gene mutation assay is based on detections of GPI-anchored protein on the cell surface of RBCs. The *Pig-A* gene is involved in the synthesis of GPI anchors that link various protein markers to the cell surface. It is known that paroxysmal nocturnal hemoglobinuria (PNH) is caused by somatic *PIG-A* mutations in hematopoietic stem cells (HSCs) and Aerolysin-resistant HSCs from a patient with PNH exhibited clonal *PIG-A* mutations (11,12). Additionally, it is considered that the absence of GPI-anchored protein of RBCs is caused by mutations occurred in the *Pig-A* gene of nucleated erythroid precursors and/or of HSCs (6). These observations suggested that expression of GPI-anchored CD24 of RBCs is depending on the *Pig-A* gene mutations happened in erythroid precursors and/or of HSCs in bone marrows. According to this, we considered that our results, shown here using peripheral blood of mice, reflected genotoxicity of C_{60} on bone marrows.

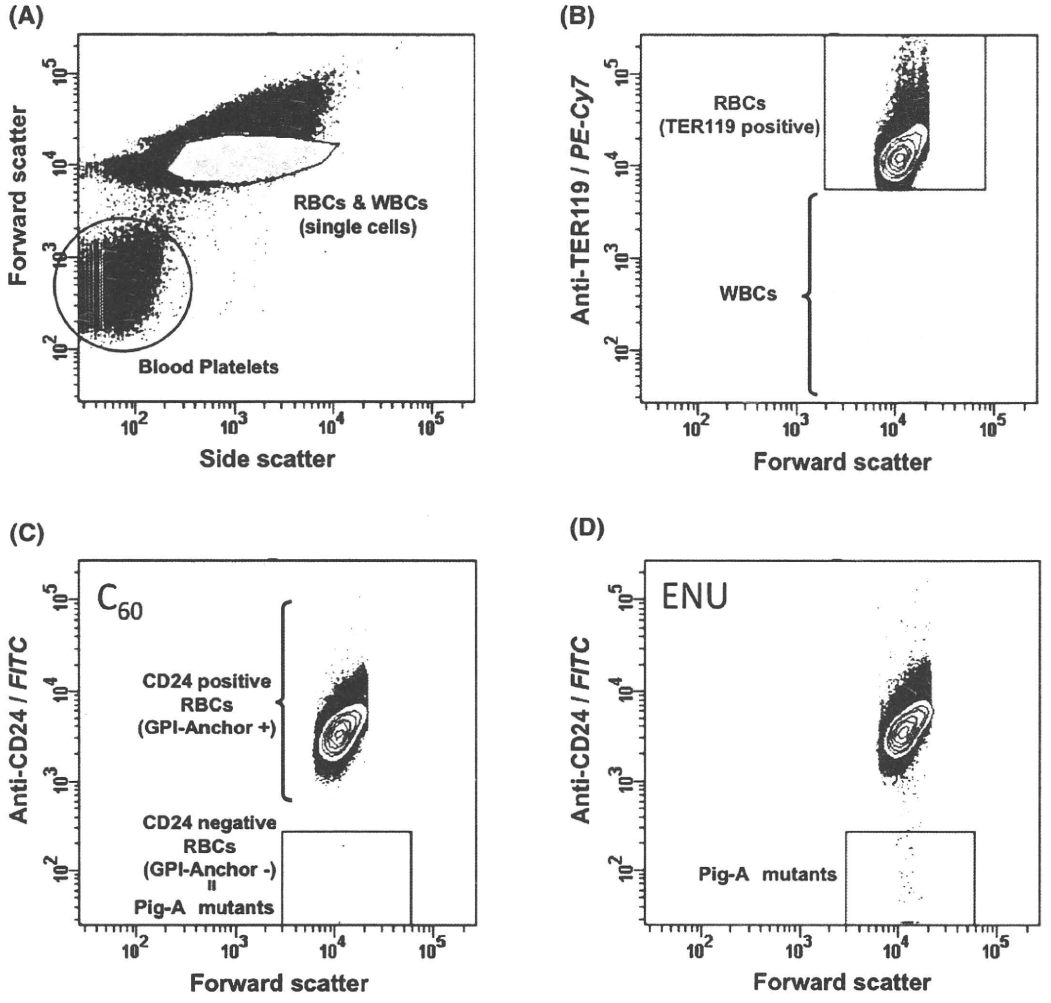

Fig. 1. Analysis of mouse peripheral blood by flow cytometry. (A) Single cell populations were gated and further analyzed with anti-TER119 antibody. (B) TER119-negative white blood cells were excluded from the gated single cell population. TER119-positive red blood cells (RBCs) were gated and further analyzed with anti-CD24 antibody. (C) Approximately 1×10^6 TER119-positive RBCs were analyzed for CD24 expression. CD24-negative RBCs (GPI-Anchor -) were scored as *Pig-A* mutants. In here, there were no obvious features in RBCs derived from C_{60} treated mice. (D) TER119-positive cells derived from ENU-treated mice were analyzed for CD24 expression.

Our data are consistent with the finding that C_{60} administered by gavage to ICR mice is negative in the *in vivo* bone marrow micronucleus test (4). These reports and our result suggest that intraperitoneal injection and gavage of C_{60} are negative for genotoxicity on bone marrow cells including erythroid precursors and HSCs. In both studies, however, the bone marrow was not exposed to C_{60} directly. A recent report showed that intratracheal instillation of C_{60} increased both mutation frequency (*gpt* assay) and DNA damage (comet assay) in the lung (3). From the mutation spectra, it was suggested that oxidative DNA damage might be involved in mutagenicity of C_{60} (3). C_{60}-phagocytized macrophages and granulomatous formations were also observed in the lung (3). Additionally, intratracheal instillation of C_{60} could induce inflammatory responses in the lung (13). It is known that reactive oxygen species (ROS) generation by nanoparticles could be due to particle-cell interactions, especially in the lungs where there is a rich pool of ROS producers like the inflammatory phagocytes, neutrophols and macrophages (14). According to these observations, it is possible that both direct exposure to the target tissue and inflammatory response are important factors in the evaluation of the genotoxicity of C_{60}.

On the other hand, details of inflammatory responses were unclear, but intraperitoneal application of C_{60} induced no obvious change on exposed area except for black patchy deposits on the serosal surfice in $p53^{+/-}$ mouse (1). Therefore it is expected that ROS generation

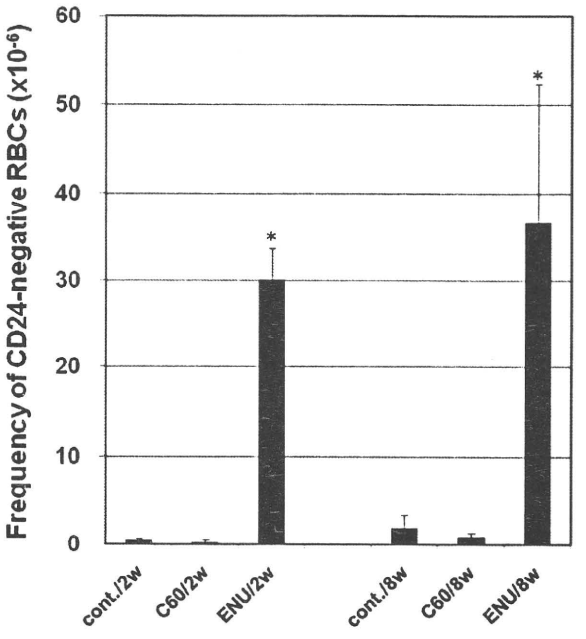

Fig. 2. Frequency of CD24-negative RBCs. At 2 and 8 weeks after mice were treated with C_{60} (3 mg/animal), ENU (40 mg/kg), or solvent, peripheral blood was withdrawn from the tail vein and RBCs were analyzed by flow cytometry for CD24 expression. Values are the mean ± SD of data from 6 animals (C_{60} and solvent) or 5 animals (ENU). *P*-values less than 0.0005 are indicated by asterisks.

by inflammatory responses might not occur and we detected negative genotoxicity in our case.

Recent reports including our results about genotoxicity of C_{60} are discrepant. However, it is known that C_{60} have an ability to quench and generate ROS (15,16). These discrepancies about genotoxicity of C_{60} may be caused by a duality of C_{60} itself. At this time, we cannot explain the mechanism(s) of C_{60} genotoxicity in detail, but we suspect that it is complex and includes oxidative DNA damages, inflammation, and other biological factors. To assess the genotoxicity of C_{60} more fully, we need a comprehensive whole body survey.

Acknowledgement: This work was supported by Health and Labor Sciences Research Grant, Japan, Grant Number: H21-chemical-general-008, and Human Science Foundation, Japan; Grant Number: KHB1006.

References

1 Takagi A, Hirose A, Nishimura T, Fukumori N, Ogata A, Ohashi N, Kitajima S, Kanno J. Induction of mesothelioma in p53$^{+/-}$ mouse by intraperitoneal application of multi-wall carbon nanotube. J Toxicol Sci. 2008; 33: 105-16.

2 Sakamoto Y, Nakae D, Fukumori N, Tayama K, Maekawa A, Imai K, Hirose A, Nishimura T, Ohashi N, Ogata A. Induction of mesothelioma by a single intrascrotal administration of multi-wall carbon nanotube in intact male Fischer 344 rats. J Toxicol Sci. 2009; 34: 65-76.

3 Totsuka Y, Higuchi T, Imai T, Nishikawa A, Nohmi T, Kato T, Masuda S, Kinae N, Hiyoshi K, Ogo S, Kawanishi M, Yagi T, Ichinose T, Fukumori N, Watanabe M, Sugimura T, Wakabayashi K. Genotoxicity of nano/microparticles in *in vitro* micronuclei, *in vivo* comet and mutation assay systems. Part Fibre Toxicol. 2009; 6: 23.

4 Shinohara N, Matsumoto K, Endoh S, Maru J, Nakanishi J. *In vitro* and *in vivo* genotoxicity tests on fullerene C_{60} nanoparticles. Toxicol Lett. 2009; 191: 289-96.

5 Miura D, Dobrovolsky VN, Kasahara Y, Katsuura Y, Heflich RH. Development of an *in vivo* gene mutation assay using the endogenous *Pig-A* gene: I. Flow cytometric detection of CD59-negative peripheral red blood cells and CD48-negative spleen T-cells from the rat. Environ Mol Mutagen. 2008; 49: 614-21.

6 Miura D, Dobrovolsky VN, Mittelstaedt RA, Kasahara Y, Katsuura Y, Heflich RH. Development of an *in vivo* gene mutation assay using the endogenous *Pig-A* gene: II. Selection of *Pig-A* mutant rat spleen T-cells with proaerolysin and sequencing *Pig-A* cDNA from the mutants. Environ Mol Mutagen. 2008; 49: 622-30.

7 Dobrovolsky VN, Shaddock JG, Mittelstaedt RA, Manjanatha MG, Miura D, Uchikawa M, Mattison DR, Morris SM. Evaluation of Macaca mulatta as a model for genotoxicity studies. Mutat Res. 2009; 673: 21-8.

8 Phonethepswath S, Bryce SM, Bemis JC, Dertinger SD. Erythrocyte-based *Pig-a* gene mutation assay: demonstration of cross-species potential. Mutat Res. 2008; 657: 122-6.

9 Miura D, Dobrovolsky VN, Kimoto T, Kasahara Y, Heflich RH. Accumulation and persistence of *Pig-A* mutant peripheral red blood cells following treatment of rats with single and split doses of *N*-ethyl-*N*-nitrosourea. Mutat Res. 2009; 677: 86-92.

10 Keller P, Tremml G, Rosti V, Bessler M. X inactivation and somatic cell selection rescue female mice carrying a Piga-null mutation. Proc Natl Acad Sci U S A. 1999; 96: 7479-83.

11 Takeda J, Miyata T, Kawagoe K, Iida Y, Endo Y, Fujita T, Takahashi M, Kitani T, Kinoshita T. Deficiency of the GPI anchor caused by a somatic mutation of the *PIG-A* gene in paroxysmal nocturnal hemoglobinuria. Cell. 1993; 73: 703-11.

12 Hu R, Mukhina GL, Piantadosi S, Barber JP, Jones RJ, Brodsky RA. *PIG-A* mutations in normal hematopoiesis. Blood. 2005; 105: 3848-54.

13 Park EJ, Kim H, Kim Y, Yi J, Choi K, Park K. Carbon fullerenes (C_{60}s) can induce inflammatory responses in the lung of mice. Toxicol Appl Pharmacol. 2010; 244: 226-33.

14 Li JJ, Muralikrishnan S, Ng CT, Yung LY, Bay BH. Nanoparticle-induced pulmonary toxicity. Exp Biol Med (Maywood). 2010; 235: 1025-33.

15 Markovic Z, Trajkovic V. Biomedical potential of the reactive oxygen species generation and quenching by

fullerenes (C_{60}). Biomaterials. 2008; 29: 3561–73.
16 Singh N, Manshian B, Jenkins GJ, Griffiths SM, Williams PM, Maffeis TG, Wright CJ, Doak SH. NanoGenotoxicology: the DNA damaging potential of engineered nanomaterials. Biomaterials. 2009; 30: 3891–914.

Carcinogenesis vol.31 no.5 pp.927–935, 2010
doi:10.1093/carcin/bgq029
Advance Access publication February 25, 2010

Involvement of macrophage inflammatory protein 1α (MIP1α) in promotion of rat lung and mammary carcinogenic activity of nanoscale titanium dioxide particles administered by intra-pulmonary spraying

Jiegou Xu[1], Mitsuru Futakuchi[1], Masaaki Iigo[1], Katsumi Fukamachi[1], David B.Alexander[1], Hideo Shimizu[2], Yuto Sakai[1,3], Seiko Tamano[4], Fumio Furukawa[4], Tadashi Uchino[5], Hiroshi Tokunaga[6], Tetsuji Nishimura[5], Akihiko Hirose[5], Jun Kanno[5] and Hiroyuki Tsuda[1,*]

[1]Department of Molecular Toxicology and [2]Core Laboratory, Nagoya City University Graduate School of Medical Sciences, 1-Kawasumi, Mizuho-cho, Mizuho-ku, Nagoya 467-8601, Japan, [3]Department of Drug Metabolism and Disposition, Graduate School of Pharmaceutical Sciences, 3-1, Tanabe-Dohri, Mizuho-ku, Nagoya 467-8603, Japan, [4]DIMS Institute of Medical Science, Inc., 64 Goura, Nishiazai, Azai-cho, Ichinomiya 491-0113, Japan, [5]National Institute of Health Sciences, 1-18-1 Kamiyoga, Setagaya-ku, Tokyo 158-8501, Japan and [6]Pharmaceuticals and Medical Devices Agency, 2-3-3, Kasumigaseki, Chiyoda-ku, Tokyo 100-0013, Japan

*To whom correspondence should be addressed. Tel: +81 52 853 8991; Fax: +81 52 853 8996;
Email: htsuda@med.nagoya-cu.ac.jp

Titanium dioxide (TiO_2) is evaluated by World Health Organization/International Agency for Research on Cancer as a Group 2B carcinogen. The present study was conducted to detect carcinogenic activity of nanoscale TiO_2 administered by a novel intrapulmonary spraying (IPS)-initiation–promotion protocol in the rat lung. Female human c-Ha-*ras* proto-oncogene transgenic rat (H*ras*128) transgenic rats were treated first with *N*-nitrosobis(2-hydroxypropyl)amine (DHPN) in the drinking water and then with TiO_2 (rutile type, mean diameter 20 nm, without coating) by IPS. TiO_2 treatment significantly increased the multiplicity of DHPN-induced alveolar cell hyperplasias and adenomas in the lung, and the multiplicity of mammary adenocarcinomas, confirming the effectiveness of the IPS-initiation–promotion protocol. TiO_2 aggregates were localized exclusively in alveolar macrophages and had a mean diameter of 107.4 nm. To investigate the underlying mechanism of its carcinogenic effects, TiO_2 was administered to wild-type rats by IPS five times over 9 days. TiO_2 treatment significantly increased 8-hydroxydeoxy guanosine level, superoxide dismutase activity and macrophage inflammatory protein 1α (MIP1α) expression in the lung. MIP1α, detected in the cytoplasm of TiO_2-laden alveolar macrophages *in vivo* and in the media of rat primary alveolar macrophages treated with TiO_2 *in vitro*, enhanced proliferation of human lung cancer cells. Furthermore, MIP1α, also detected in the sera and mammary adenocarcinomas of TiO_2-treated H*ras*128 rats, enhanced proliferation of rat mammary carcinoma cells. These data indicate that secreted MIP1α from TiO_2-laden alveolar macrophages can cause cell proliferation in the alveoli and mammary gland and suggest that TiO_2 tumor promotion is mediated by MIP1α acting locally in the alveoli and distantly in the mammary gland after transport via the circulation.

Introduction

Inhalation of particles and fiber is well known to be strongly associated with increased lung cancer risk in the workplace (1,2). Although the size of fiber particles was reported to be closely related to risk (3), the precise role of particles and fibers in lung cancer induction has not yet been elucidated.

Titanium dioxide (TiO_2) particles of various sizes are manufactured worldwide in large quantities and are used in a wide range of applications. TiO_2 particles have long been considered to pose little risk to respiratory health because they are chemically and thermally stable. However, TiO_2 is classified as a Group 2B carcinogen, a possible carcinogen to humans, by World Health Organization/International Agency for Research on Cancer based on the findings of lung tumor induction in female rats (3,4). This overall evaluation includes nanoscale (<100 nm in diameter) and larger sized classes of TiO_2. At present, the mechanism underlying the development of rat lung tumors by inhalation of TiO_2 particles is unclear.

Inhalation of TiO_2 particles can occur both at the workplace, e.g. in manufacturing and packing sites, and also outside the workplace during their use (5–7). Exposure to airborne nanoparticles has been reported to be associated with a granulomatous inflammatory response in the lung (8). Inhalation studies of nanoparticles for cancer risk assessment is urgently needed, however, due to the high cost of long-term studies, available data is severely limited (9,10). The aim of this study is to understand the mechanism underlying rat lung carcinogenesis induced by inhalation of TiO_2 particles. We choose intrapulmonary spraying (IPS) because it does not require costly facilities, allows accurate dose control and approximates long-term inhalation studies (3,11).

We initially examined whether TiO_2 particles have carcinogenic activity in the rat lung using a novel IPS-initiation–promotion protocol (12,13). For these experiments, Sprague–Dawley (SD)-derived female human c-Ha-*ras* proto-oncogene transgenic rat (H*ras*128) transgenic rats, which are known to have the same carcinogen susceptibility phenotype in the lung as wild-type rats but are highly susceptible to mammary tumor induction (14–16), were treated with *N*-nitrosobis(2-hydroxypropyl)amine (DHPN) to initiate carcinogenesis and then treated with TiO_2 by IPS. We observed a promotion effect of TiO_2 particles in lung and mammary gland carcinogenesis.

To identify factors involved in this promotion effect, wild-type SD strain rats were treated with TiO_2 by IPS for 9 days. We found macrophage inflammatory protein 1α (MIP1α) was produced by TiO_2-laden alveolar macrophages in the lungs of rats treated with TiO_2. MIP1α is a member of the CC chemokine family and is primarily associated with cell adhesion and migration of multiple myeloma cells (17). It is reported to be produced by macrophages in response to a variety of inflammatory stimuli including TiO_2 (18). In the present study, MIP1α, detected in the medium of rat primary alveolar macrophages treated with TiO_2, enhanced proliferation of human lung cancer cells *in vitro*. MIP1α was also detected in the sera and mammary adenocarcinomas of TiO_2-treated H*ras*128 rats and enhanced proliferation of rat mammary carcinoma cells.

Materials and methods

Animals

Female transgenic rats carrying the H*ras*128 and female wild-type SD rats were obtained from CLEA Japan Co., Ltd (Tokyo, Japan) (15). The animals were housed in the animal center of Nagoya City University Medical School, maintained on a 12 h light–dark cycle and received Oriental MF basal diet (Oriental Yeast Co., Tokyo, Japan) and water *ad libitum*. The research was conducted according to the Guidelines for the Care and Use of Laboratory Animals of

Abbreviations: CCR1, C-C chemokine receptor type 1; DHPN, *N*-nitrosobis (2-hydroxypropyl) amine; ERK, extracellular signal-regulated kinase; GRO, growth-regulated oncogene; H*ras*128 rat, human c-Ha-*ras* proto-oncogene transgenic rat; IL, interleukin; IPS, intrapulmonary spraying; MEK1, MAPK/ERK kinase1; MIP1α, macrophage inflammatory protein 1α; 8-OHdG, 8-hydroxydeoxy guanosine; PBS, phosphate-buffered saline; ROS, reactive oxygen species; SD, Sprague–Dawley; SOD, superoxide dismutase; TEM, transmission electron microscopy; TiO_2, titanium dioxide.

Nagoya City University Medical School and the experimental protocol was approved by the Institutional Animal Care and Use Committee (H17-28).

Preparation of TiO_2 and IPS

TiO_2 particles (rutile type, without coating; with a mean primary size of 20 nm) were provided by Japan Cosmetic Association, Tokyo, Japan. TiO_2 particles were suspended in saline at 250 μg/ml or 500 μg/ml. The suspension was autoclaved and then sonicated for 20 min just before use. The TiO_2 suspension was intratracheally administered to animals under isoflurane anesthesia using a Microsprayer (Series IA-1B Intratracheal Aerosolizer, Penn-Century, Philadelphia, PA) connected to a 1 ml syringe; the nozzle of the sprayer was inserted into the trachea through the larynx and a total of 0.5 ml suspension was sprayed into the lungs synchronizing with spontaneous respiratory inhalation (IPS).

IPS-initiation–promotion protocol

Thirty-three female H*ras*128 rats aged 6 weeks were given 0.2% DHPN, (Wako Chemicals Co., Ltd Osaka, Japan) in the drinking water for 2 weeks and 9 rats were given drinking water without DHPN. Two weeks later, the rats were divided into four groups, DHPN alone (Group 1), DHPN followed by 250 μg/ml TiO_2 (Group 2), DHPN followed by 500 μg/ml TiO_2 (Group 3) and 500 μg/ml TiO_2 without DHPN (Group 4). The TiO_2 particle preparations were administered by IPS once every 2 weeks from the end of week 4 to week 16 (a total of seven times). The total amount of TiO_2 administered to Groups 1, 2, 3 and 4 were 0, 0.875, 1.75 and 1.75 mg per rat, respectively. Three days after the last treatment, animals were killed and the organs (brain, lung, liver, spleen, kidney, mammary gland, ovaries, uterus and neck lymph nodes) were excised and divided into two pieces; one piece was immediately frozen at −80°C and used for quantitative measurement of elemental titanium, and the other piece was fixed in 4% paraformaldehyde solution in phosphate-buffered saline (PBS) buffer adjusted to pH 7.3 and processed for light microscopic examination and transmission electron microscopy (TEM); the left lungs and inguinal mammary glands were used for elemental titanium analysis and the right lungs and inguinal mammary glands were used for microscopic examination.

IPS 9 day protocol

Twenty female SD rats (wild-type counterpart of H*ras*128) aged 10 weeks were treated by IPS with 0.5 ml suspension of 500 μg/ml TiO_2 particles in saline five times over a 9 day period (Figure 2A). The total amount of TiO_2 administered was 1.25 mg per rat. Six hours after the last dose, animals were killed and the lungs and inguinal mammary glands were excised. Fatty tissue surrounding the mammary gland was removed as much as possible. The left lungs and inguinal mammary glands were used for biochemical analysis, and the right lungs were fixed in 4% paraformaldehyde solution in PBS adjusted at pH 7.3 and processed for histopathological examination and immunohistochemistry.

Light microscopic and TEM observation of TiO_2 particles in the lung

Paraffin blocks were deparaffinized and embedded in epon resin and processed for TiO_2 particle observation and titanium element analysis, using a JEM-1010 transmission electron microscope (JEOL Co. Ltd, Tokyo, Japan) equipped with an X-ray microanalyzer (EDAX, Tokyo, Japan). Size analysis of TiO_2 particles was performed using TEM photos by an image analyzer system, (IPAP, Sumika Technos Corporation, Osaka, Japan). A total of 452 particles from alveolar macrophages from rats in Group 3 (DHPN followed by 500 μg/ml TiO_2) of the IPS-initiation–promotion study and a total of 2571 particles from alveolar macrophages from rats in the IPS 9 day study were measured.

Biochemical element analysis of titanium

For the detection of elemental titanium, frozen tissue samples of 50–100 mg were digested with 5 ml concentrated HNO_3 for 22 min in a microwave oven. Titanium in the digested solutions was determined by inductively coupled plasma–mass spectrometry (HP-4500, Hewlett-Packard Co., Houston, TX) under the following conditions: RF power, 1450 W; RF refraction current, 5 W; Plasma gas current, 15 l/min; Carrier gas current, 0.91 l/min; Peri pump, 0.2 r.p.s.; Monitoring mass-m/z 48 (Ti); Integrating interval, 0.1 s; Sampling period 0.31 s.

Analysis of superoxide dismutase activity, 8-hydroxydeoxy guanosine and cytokine levels

For the analysis of superoxide dismutase (SOD) activity, 8-hydroxydeoxy guanosine (8-OHdG) and cytokine levels, animals exposed to TiO_2 particles for 9 days were used. For 8-OHdG levels, genomic DNA was isolated from the left lung and inguinal mammary gland with a DNA Extractor WB Kit (Wako Chemicals Co. Ltd). 8-OHdG levels were determined with an 8-OHdG ELISA Check Kit (Japan Institute for the Control of Aging, Shizuoka, Japan) and by a custom service (OHG Institute Co., Ltd, Fukuoka, Japan). For the analysis of SOD activity and inflammation-related cytokines, tissue from the left lung and inguinal mammary glands was excised and rinsed with cold PBS three times and homogenized in 1 ml of T-PER, Tissue Protein Extraction Reagent (Pierce, Rockford, IL), containing 1% (vol/vol) proteinase inhibitor cocktail (Sigma–Aldrich, St Louis, MO). The homogenates were clarified by centrifugation at 10 000*g* for 5 min at 4°C. Protein content was measured using a BCA™ Protein Assay Kit (Pierce). SOD activity was determined using an SOD Assay Kit (Cayman Chemical Co., Ann Arbor, MI). The levels of interleukin (IL)-1α, IL-1β, IL-6, granulocyte-macrophage colony-stimulating factor, granulocyte colony-stimulating factor, tumor necrosis factor α, interferon γ, IL-18, monocyte chemotactic protein 1 and MIP1α, growth-regulated oncogene (GRO) and vascular endothelial growth factor were measured by Multiplex Suspension array (GeneticLab Co., Ltd, Sapporo, Japan).

Immunohistochemistry

CD68 and MIP1α were detected using anti-rat CD68 (BMA Biomedicals, Augst, Switzerland) and anti-rat MIP1α polyclonal antibodies (BioVision, Lyon, France). Both antibodies were diluted 1:100 in blocking solution and applied to slides, and the slides were incubated at 4°C overnight. The slides were then incubated for 1 h with biotinylated species-specific secondary antibodies diluted 1:500 (Vector Laboratories, Burlingame, CA) and visualized using avidin-conjugated alkaline phosphatase complex (ABC kit, Vector Laboratories) and Alkaline Phosphatase Substrate Kit (Vector Laboratories).

Isolation of primary alveolar macrophages and preparation of conditioned media

Wild-type female SD rats were given 0.5 ml 6% thioglycollate medium (Thioglycollate Medium II, Eiken Chemical Co., Ltd, Tokyo, Japan) by IPS on days 1, 3 and 5, and 6 h after the last treatment, the lungs were excised and minced with sterilized scissors in RPMI 1640 containing 10% fetal bovine serum (Wako Chemicals Co., Ltd) and antibiotics. The homogenate was washed twice and plated onto 6 cm dishes and incubated for 2 h at 37°C, 5% CO_2. The dishes were then washed with PBS three times to remove unattached cells and cell debris. Samples of the remaining adherent cells were cultured in chamber slides and immunostained for CD68 to confirm their identity as macrophages; ~98% of the cells were positive for CD68.

Primary alveolar macrophages were treated with vehicle or TiO_2 particles in saline suspension at a final concentration of 100 μg/ml and then incubated for 24 h in a 37°C, 5% CO_2 incubator. The conditioned medium was collected and diluted 5-fold with RPMI 1640; the conditioned medium had a final concentration of 2% fetal bovine serum.

Western blotting

For the detection of MIP1α, aliquots of 20 μg protein from the extracts of lung or mammary tissue were separated by 15% sodium dodecyl sulfate–polyacrylamide gel electrophoresis, transferred to nitrocellulose membranes and immunoblotted. For the detection of C-C chemokine receptor type 1 (CCR1), 10% sodium dodecyl sulfate–polyacrylamide gel electrophoresis was used for the separation. Membranes were probed overnight at 4°C with anti-rat MIP1α polyclonal antibody (BioVision) diluted at 1:100 or anti-CCR1 (Santa Cruz Biotechnology, Santa Cruz, CA) diluted at 1:100. The blots were washed and incubated for 1 h with biotinylated anti-species-specific secondary antibodies (Amersham Biosciences, Piscataway, NJ) and then visualized using ECL Western Blotting Detection Reagent (Amersham Biosciences). To ensure equal protein loading, the blots were striped with Restore Western Blot Stripping Buffer (Pierce) and reprobed with anti-β actin antibody (dilution 1:2000; Sigma–Aldrich) for 1 h at room temperature.

For the detection of serum MIP1α, GRO and IL-6, aliquots of 150 μg of protein from the sera of rats treated with TiO_2 for 16 weeks were subjected to sodium dodecyl sulfate–polyacrylamide gel electrophoresis. Anti-human GRO polyclonal antibody (BioVision) and anti-mouse IL-6 polyclonal antibody (Santa Cruz) were diluted 1:100. For detection of activated extracellular signal-regulated kinase (ERK) 1/2 and total ERK1/2, phospho ERK1/2 antiboby (Cell signaling Technology, Beverly, MA) and ERK1/2 antibody (Upstate, Lake placid, NY) were diluted 1:2000 and 1:25 000, respectively. The conditioned medium from alveolar macrophages, prepared as described above, was also subjected to western blot assay for MIP1α detection as described above. The blots were striped with Restore Western Blot Stripping Buffer (Pierce) and stained with Ponceau S solution (Sigma–Aldrich) for 10 min. The major band at 66 kDa was judged to be albumin and used as an internal control.

In vitro cell proliferation assay

A549 cells, a human lung cancer cell line, and the rat mammary cancer cell line C3 (19), derived from the H*ras*128 transgenic rats, were used in the *in vitro* cell proliferation assays. A549 or C3 cells were seeded into 96-well culture plates at 5×10^3 cells per well in 2% fetal bovine serum Dulbecco's modified Eagle's medium (Wako Chemicals Co., Ltd). After overnight incubation, the cells were treated as noted below, incubated for 72 h and the relative cell number was then determined.

To investigate the effect of culture supernatant from alveolar macrophages on A549 cell proliferation, their media were replaced with diluted conditioned medium, and the cells were incubated for 72 h with 0, 5, 10 and 20 μg/ml of anti-MIP1α neutralizing antibody (R&D Systems, Minneapolis, MN) or with 20 μg/ml of irrelevant IgG. To investigate the effect of recombinant cytokines on A549 cell proliferation, 10, 50 or 100 ng/ml of recombinant protein, rat MIP1α (R&D Systems), human GRO (R&D Systems) or human IL-6 (R&D Systems), was added to A549 cells. To investigate the role of ERK in MIP1α-stimulated cell proliferation, A549 cells, treated with or without 2×10^{-7} M of the specific MAPK/ERK kinase1 (MEK1) inhibitor PD98059 (Cell Signaling Technology) for 10 min, were treated with 50 ng/ml of MIP1α protein. To investigate the effect of reactive oxygen species (ROS) on cell proliferation, A549 cells, with or without pretreatment with 1 mM *N*-acetyl cysteine (Wako Chemicals Co. Ltd) for 30 min, were treated with 0.5 mM H_2O_2 (Wako Chemicals Co. Ltd). To investigate of the effects of MIP1α on rat mammary cells, C3 cells were treated with serially diluted recombinant rat MIP1α (0, 0.4, 2.0, 10 and 50 ng/ml, respectively; R&D Systems). For detecting the direct effect of TiO_2 particles on A549 and C3 cell proliferation, 5×10^3 A549 or C3 cells were cultured overnight and then treated with 10 or 50 μg/ml of TiO_2 particles.

After 72 h incubation, the relative cell number of A549 and C3 was determined using the Cell Counting Kit-8 (Dojindo Molecular Technologies, Rockville, MD) according to the manufacturer's instruction.

Statistical analysis

For *in vivo* data, statistical analysis was performed using the Kruskal–Wallis and Bonferroni–Dunn's multiple comparison tests. *In vitro* data are presented as means ± standard deviations. The statistical significance of *in vitro* findings was analyzed using a two-tailed Student's *t*-test and Bonferroni–Dunn's multiple comparison tests. A value of $P < 0.05$ was considered significant. The Spearman's rank correlation test was used to determine the association between TiO_2 dose and TiO_2 carcinogenic activity.

Results

Promoting effects of TiO_2 particles in DHPN-induced lung and mammary carcinogenesis

Prior to initiation of the IPS-initiation–promotion and IPS 9 day studies, we conducted a preliminary study to confirm whether IPS would be a good tool to deliver TiO_2 particles to the alveoli. Rats were treated by IPS with India ink. We observed that ink particles of ~50 to 500 μm in diameter were diffusely distributed throughout the alveoli space (data not shown), confirming that IPS could deliver TiO_2 particles to the alveoli.

Four groups of female H*ras*128 rats were treated with +/− DHPN to initiate carcinogenesis and then treated with TiO_2 by IPS for 12 weeks: Group 1, DHPN alone; Group 2, DHPN followed by 250 μg/ml TiO_2; Group 3, DHPN followed by 500 μg/ml TiO_2 and Group 4, 500 μg/ml TiO_2 without DHPN. Microscopic observation in the lung showed scattered inflammatory foci, alveolar cell hyperplasia (Figure 1A) and adenomas in the DHPN-treated rats. The multiplicity (numbers per square centimeter lung) of hyperplasias and adenomas in Group 3 (DHPN followed by 500 μg/ml TiO_2) were significantly increased compared with Group 1 (DHPN followed by saline, Table I), and the increase showed a dose-dependent correlation (rho = 0.630, $P = 0.001$ for hyperplasias and rho = 0.592, $P = 0.029$ for adenomas) by the Spearman's rank correlation test. In the mammary gland, TiO_2 treatment significantly increased the multiplicity of adenocarcinomas (Figure 1C) and tended to increase the weight of the mammary tumors (Figure 1C). In the rats, which received TiO_2 treatment without prior DHPN treatment, alveolar proliferative lesions were not observed although slight inflammatory lesions were observed.

TiO_2 was distributed primarily to the lung, but minor amounts of TiO_2 were also found in other organs (supplementary Figure 1A is available at *Carcinogenesis* Online).

Various sizes of TiO_2 aggregates were observed in alveolar macrophages (Figure 1B). The TiO_2-laden macrophages were evenly scattered throughout the lung alveoli. The number of hyperplasias with TiO_2-laden macrophages was dose dependently increased (supplementary Table 1 is available at *Carcinogenesis* Online). This result suggests that TiO_2-laden macrophages may be involved in the promotion of alveolar hyperplasia.

The size distribution of TiO_2 particle aggregate is shown in Figure 1D. Of 452 particle aggregates examined, 362 (80.1%) were nanosize, i.e. <100 nm. Overall, the average size was 84.9 nm and the median size was 44.4 nm.

IPS 9 day study—analysis of TiO_2

Female SD rats were treated with TiO_2 by IPS over a 9 day period (Figure 2A). Microscopic observation showed scattered inflammatory lesions with infiltration of numerous macrophages mixed with a few neutrophils and lymphocytes in TiO_2-treated animals. Overall, the number of macrophages in the alveoli was significantly increased in the TiO_2-treated animals (Figure 2B). As expected from the results of the IPS-initiation–promotion study, alveolar proliferative lesions were not observed (Figure 2C).

Morphologically, TiO_2 particles were observed as yellowish, polygonal bodies in the cytoplasm of cells (Figure 2D). These cells are morphologically distinct from neutrophils and strongly positive for CD68 (Figure 2E), indicating that the TiO_2 engulfing cells were macrophages. TiO_2 aggregates of various sizes were found in macrophages, and aggregates larger than a single macrophage were surrounded by multiple macrophages (supplementary Figure 1B is available at *Carcinogenesis* Online)

TEM also showed electron dense bodies in the cytoplasm of macrophages (Figure 2F and G). These bodies were found exclusively in macrophages and not found in the alveolar parenchyma, including alveolar epithelium and alveolar wall cells, or in any other cell type. The shape of the electron dense TiO_2 particles in the cytoplasm was quite similar to that observed in preparations taken from TiO_2 suspensions before administration (Figure 2H and supplementary Figure 1C and D is available at *Carcinogenesis* Online). Individual TiO_2 particles were rod-like in shape (supplementary Figure 1C is available at *Carcinogenesis* Online).

Element analysis by TEM and X-ray microanalysis indicated that these electron dense bodies were composed primarily of titanium particles (supplementary Figure 1E and F-1 and 1F-2 is available at *Carcinogenesis* Online). Titanium was not observed in the surrounding alveolar cells without electron dense bodies (supplementary Figure 1F-3 is available at *Carcinogenesis* Online). The size distribution of TiO_2 particle aggregates is shown in Figure 2I. Of 2571 particle aggregates examined, 1970 (76.6%) were <100 nm and five particles were >4000 nm in size. Overall, the average size was 107.4 nm and the median size was 48.1 nm.

IPS 9 day study—analysis of oxidative stress and inflammation-related factors in the lungs of wild-type rats

IPS of TiO_2 particles significantly increased SOD activity (Figure 3A) and 8-OHdG levels (Figure 3B) in the lungs of wild-type rats, but not in the mammary glands. Analysis of the expression levels of 12 cytokines using suspension array indicated that administration of TiO_2 particles significantly upregulated the expression of MIP1α, GRO and IL-6 in the lung tissue of wild-type rats (supplementary Table 2 is available at *Carcinogenesis* Online). MIP1α levels were slightly elevated (0.4 pg/mg protein) in the mammary gland (Figure 3C), although the elevation was not statistically significant. Elevation of MIP1α in the lung tissue of animals treated with TiO_2 particles was confirmed by western blotting (Figure 3D).

Immunohistochemically, MIP1α was detected in the cytoplasm of alveolar macrophages with phagocytosed TiO_2 particles (Figure 3E upper, stained in red) and these macrophages could be found in hyperplastic lesions of the lung (supplementary Figure 2A and B is available at *Carcinogenesis* Online). MIP1α was not detected in macrophages without TiO_2 particles (Figure 3E lower). Expression of CCR1, the major receptor of MIP1α, was observed in the lung; IPS of TiO_2 particles had little or no effect on CCR1 expression (supplementary Figure 2C is available at *Carcinogenesis* Online).

Effect of MIP1α on proliferation of a human lung cancer cell line in vitro

Alveolar macrophages were isolated from the lungs of SD rats and were confirmed to be macrophages by morphology and CD68 staining